

## Nanoscopic insight into acrylic acid gelation using low-field RheoNMR

Christian Fengler<sup>1</sup>, Jonas Keller<sup>1</sup>, Karl-Friedrich Ratzsch<sup>2</sup>, and Manfred Wilhelm<sup>1</sup><sup>1</sup>Institute for Chemical Technology and Polymer Chemistry, Karlsruhe Institute of Technology, Karlsruhe, Germany<sup>2</sup>Bruker Biospin GmbH, Rheinstetten, Germany

## ABSTRACT

The aqueous acrylic acid (AAc) solution polymerization was studied using a unique low-field RheoNMR device that couples oscillatory shear rheology with time-domain NMR relaxometry (TD-NMR) measurements. This coupling allows for an in-situ correlation of the elastic response with the characteristic transverse magnetization decay curve during the polymerization, adding a molecular observable to the macroscopic rheological data. TD-NMR measurements are further exploited as a concentration probe, which is used to monitor the polymer concentration dependency of  $G'$  during gelation. We found that  $G'$  is proportional to the concentration with a characteristic scaling exponent of 2.3, which is in agreement with theoretical predictions of  $G'$  based on polymer dynamics in semi-dilute entangled polymer solutions.

## INTRODUCTION

Gelation describes a process of molecules that connect to a three-dimensional network. The junctions between molecules inside the network consist of either covalent bonds or physical associations such as hydrogen bonds, entanglements, crystalline domains and electrostatic interactions. The mechanical properties of the formed gel are consequently a result of their molecular architecture, which drives the need for a fundamental understanding of the relationship between molecular structure and

macroscopic properties. Rheology has been extensively used to study gelation processes, yet it lacks a molecular dimension.<sup>1,2</sup> In contrast, TD-NMR is a versatile, non-invasive technique that studies molecular dynamics from which topological characteristics and the composition of materials can be inferred. Successful TD-NMR applications are, for instance, the quantification of crosslink densities as well as network heterogeneity in elastomers,<sup>3,4</sup> the investigation of crystallization kinetics in polymers and fats,<sup>5-7</sup> and quality control in food science.<sup>8</sup> To gain a more comprehensive insight into the relation between molecular properties and the viscoelastic response, we developed a unique portable <sup>1</sup>H NMR unit (25 MHz Larmor frequency) that can be integrated into high-end rheometers, as shown in Fig. 1.

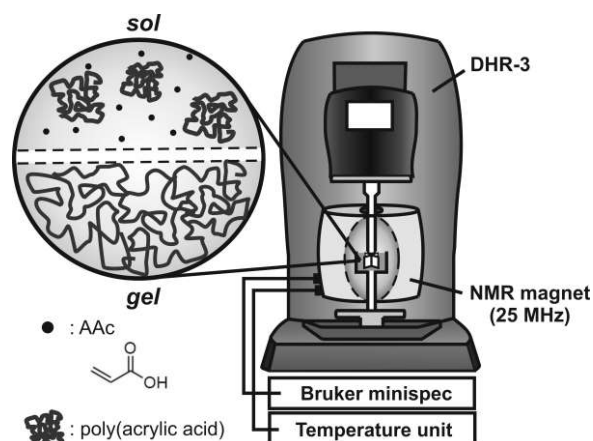


Figure 1. Low-field RheoNMR device used for monitoring the free radical solution polymerization and gelation of AAc.

## EXPERIMENTAL

### Materials

Deuterium oxide (D<sub>2</sub>O, 99 %) and 2,2'-azobis [2-(2-imidazolin-2-yl) propane] dihydrochloride (VA-044, 95 %). Acrylic acid (AAc, >99 %) was freshly distilled before synthesis.

### Synthesis

Poly(acrylic acid) gels were prepared by aqueous solution polymerization using a 20 wt% AAc solution in D<sub>2</sub>O and VA-044 as initiator. First, D<sub>2</sub>O (12.4 g) was added to AAc (3.6 g, 0.05 mol). The initiator VA-044 (0.018 g, 0.06 mmol) was separately dissolved in 2 g D<sub>2</sub>O and added to the reaction mixture. The solution was cooled to 0 °C and 0.8 mL were poured into the cup geometry.

### RheoNMR setup

The centerpiece of the RheoNMR device is a portable low field <sup>1</sup>H NMR unit ( $B_0 = 0.6$  T, 25 MHz Larmor frequency) that is integrated into a DHR-3 rheometer (TA Instruments). The NMR magnet consists of a Halbach array of NdFeB permanent magnets. For the detailed technical layout of the construction, see previous work.<sup>5</sup> The NMR probe has a dead time of 10  $\mu$ s and pulse lengths of 2.2  $\mu$ s (90°) and 4.4  $\mu$ s (180°). The Bruker “the minispec” electronic unit (NF series) was used for data acquisition and pulsing. Sample temperature was controlled by a Bruker VTU unit to 40 °C at an air flow rate of 270 L h<sup>-1</sup>.

### Rheology

The gelation was monitored by oscillatory time sweeps at a constant nominal strain  $\gamma_0 = 0.5$  % and an angular frequency  $\omega = 6.8$  rad s<sup>-1</sup>, which was found to be in the linear viscous regime of a gelled sample via a strain sweep in the range of  $\gamma_0 = 0.5$  % to 300 % at  $\omega = 6.8$  rad s<sup>-1</sup>. A vane (4 blades with diameter: 8 mm, height: 11 mm, width:

1.2 mm) and a cup (diameter: 11 mm, height: 13 mm) made out of poly(chlorotrifluoroethylene) (PCTFE) was used as the geometry to maximize sample volume. The distance of the vane to the bottom of the cup was kept constant at 1 mm.

### Time-domain NMR

The transverse magnetization decay was measured in-situ using <sup>1</sup>H  $T_2$  relaxation measurements with a combined MSE (magic sandwich echo)-CPMG/XX4 (Carr, Purcell, Meiboom, Gill) pulse sequence.<sup>5,4,9,10</sup> The MSE consists of 90° pulses and refocuses the transverse magnetization over the dead time, determining the signal intensity at  $t_{\text{NMR}} = 0$  ms.<sup>11</sup> The CPMG/XX4 pulse sequence refocuses the transverse magnetization with a delay of  $2\tau_{\text{CPMG}} = 100$   $\mu$ s between 180° pulses.

The combined pulse sequence ends with a recycle delay (RD) of 300 ms, which is 5 times higher than the longitudinal relaxation ( $T_1$ ) of the polymer ( $T_{1,\text{poly}} = 40$  ms), measured by a saturation recovery experiment.<sup>4</sup> Therefore, the chosen RD works as a  $T_1$  filter, ensuring the quantitative determination of the polymer while simultaneously suppressing the signal of mobile low molecular weight (solvent as HDO, monomer) components with a  $T_1$  times in the range of seconds.

For signal averaging, 8 scans were used that results in a duration of 5 seconds per NMR  $T_2$  experiment, ensuring a sufficient time resolution to study the gelation.

## RESULTS AND DISCUSSION

Rheology measures a macroscopic property and is not able to provide molecular information on the nanoscopic scale. This lack of a molecular dimension is resolved by conducting simultaneously TD-NMR experiments. In-situ <sup>1</sup>H  $T_2$  relaxation measurements are used to determine the time-evolution of the characteristic transverse magnetization decay during gelation. The exponential time constant of

this decay is referred to as  $T_2$  relaxation time and is related to the homonuclear dipolar coupling of neighbouring (0.2-2 nm)  $^1\text{H}$  spins along the polymer backbone. The strength of this coupling is proportional to the segmental motion (<10 nm) of the polymer backbone. At fast motions such as in a diluted polymer solution, this coupling is mostly averaged to zero and a long  $T_2$  relaxation time in the order of seconds observed. A solid state exhibits a stronger dipolar coupling and short  $T_2$  times in the order of milliseconds are measured.

Hence, TD-NMR is able to quantify the heterogeneity of a sample based on differences in the molecular motion from which topological characteristics can be

inferred. The transverse relaxation is evaluated by a stretched exponential according to

$$I(t_{\text{NMR}}) = A \exp\left(-\left(\frac{t_{\text{NMR}}}{T_2}\right)^\beta\right) + \text{offset}, \quad (1)$$

where  $\beta$  is the stretching exponent,  $T_2$  is the transverse relaxation time and the offset is set to 1 a.u., as shown in Fig. 2a. The stretched exponential fit to the transverse magnetization decay reveals a constant stretching exponent  $\beta = 0.9$  beyond a  $G'$  of 100 Pa (not shown).

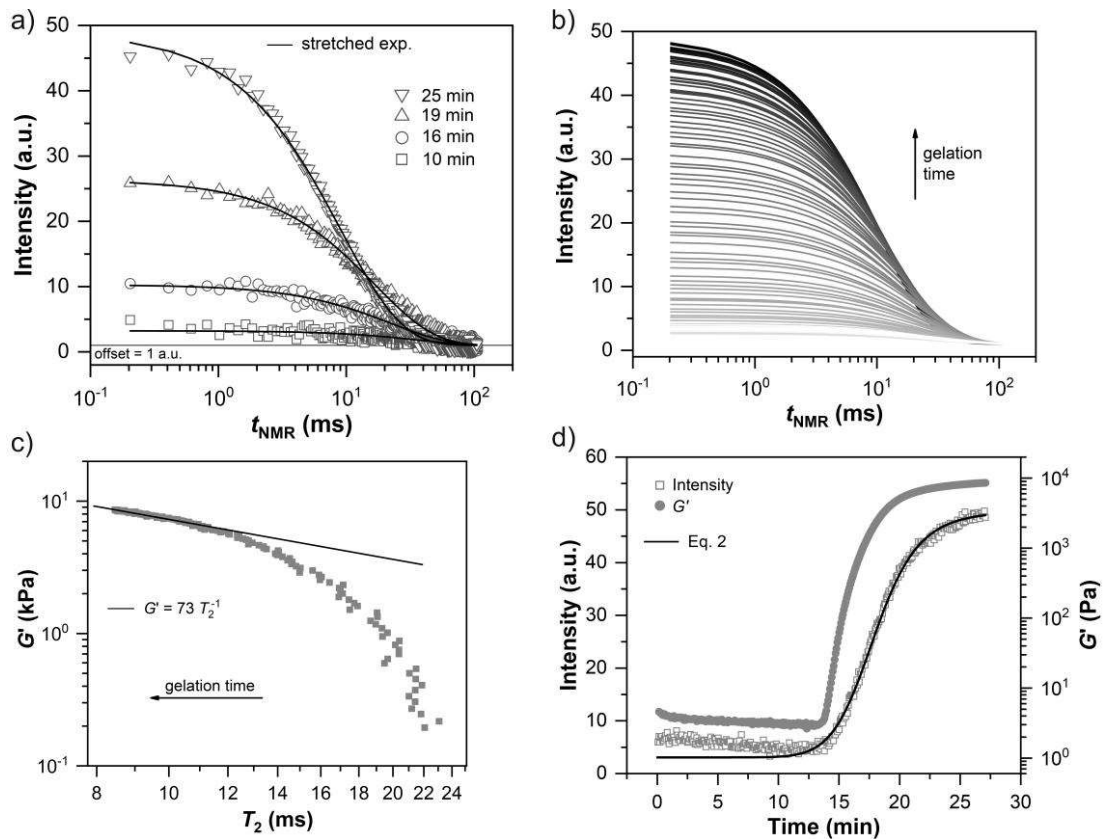


Figure 2. a) Transverse relaxation curves at different AAc gelation times obtained by a combined MSE-CPMG/XX4 pulse sequence. Solid lines are least-squares fits using a stretched exponential function (see Eq. 1). b) Stretched exponential fits throughout the gelation process. c) Direct correlation of  $G'$  with  $T_2$  times, displayed on a log-log scale. The  $T_2$  time approaches an inverse relationship with  $G'$ , illustrated by the solid line with a prefactor = 73 kPa ms. d) Time-evolution of the initial ( $t_{\text{NMR}} = 0$  ms) signal intensity and the elastic modulus. Both curves show a similar sigmoidal behavior. Solid line represents a least-squares fit according to Eq. 2 to describe the NMR gelation kinetics.

Hence, this almost monoexponential decay with a characteristic  $T_2$  time suggests a uniform distribution of constraints formed by the physical entanglements as well as the highly mobile nature of the polymer segments. This is expected considering the semi-dilute entangled state of the sample (20 wt% assuming full conversion of AAc). In contrast, for highly crosslinked samples such as rubbers above the glass transition temperature, the transverse magnetization decay is dominated by the residual dipolar coupling of the crosslinks, leading to a compressed exponential behaviour where  $\beta$  is in the range of 1 to 2.<sup>12,3</sup>

The direct correlation of  $G'$  with the  $T_2$  time is shown in Fig. 2c. At low  $G'$  values around 200 Pa, a  $T_2$  time of 20 ms is observed and can be associated with the segmental motion of the PAAc backbone. As the polymerization proceeds and additional constraints via physical entanglements are introduced into the network, the dependence of  $G'$  on  $T_2$  approaches an inverse relationship ( $G' = 73T_2^{-1}$ ). Since  $G'$  is directly proportional to the network strand number density ( $\nu$ ) times  $kT$ , this approach towards the inverse dependency indicates a critical threshold around 6 kPa at which the segmental motion of the polymer backbone becomes dominantly influenced by the number density of entangled strands ( $T_2^{-1} \sim \nu kT$ ).

The time-evolution of the NMR signal intensity and  $G'$  is shown in Fig. 2d. During the polymerization of AAc, the sample transitions from a liquid, low viscous state to a solid gel-like state. This transition is reflected in the NMR data. Since a  $T_1$  filter is used to suppress the contribution of mobile low molecular weight components such as monomer and HDO solvent, a low signal intensity of approximately 6 a.u. is observed in the liquid state at early gelation times up to 13 min. Subsequently, the signal intensity rises distinctly up to almost 50 a.u. beyond

the gel point, which is indicated by the distinct increase of  $G'$  (see Fig. 2d). During the polymerization,  $G'$  rises rapidly over several orders of magnitude from 3 Pa to 9000 Pa.

Both NMR and rheological data show the similar sigmoidal curve behaviour with three characteristic phases: i) an induction period, ii) a rapid increase of  $G'$  and NMR signal intensity, iii) an approach to a plateau value. The measured modulus of 3 Pa in the induction period is attributed to the inertia of the vane geometry as indicated by the 180° raw phase angle and represents the limit in sensitivity (1.6  $\mu\text{N m}$ ) of the used setup.

As the NMR signal intensity is related to the number of spins inside the probe volume, the RheoNMR approach allows for monitoring the polymer concentration during the polymerization. To deduct the contribution of solvent to the signal, the time-evolution of the signal intensity is first evaluated by the following fitting function

$$I(t) = \frac{(I_{\max} - I_{\text{solv}})t^m}{t^m + \theta_{\text{NMR}}^m} + I_{\text{solv}}, \quad (2)$$

where  $I_{\max}$  is the maximum signal intensity,  $\theta_{\text{NMR}}$  is the gelation half time with  $I(\theta_{\text{NMR}}) = 0.5I_{\max}$ ,  $m$  is the gelation rate exponent and  $I_{\text{solv}}$  the residual solvent signal (see Fig. 2d). The NMR data is renormalized according to

$$c_{\text{rel}} = \frac{I - I_{\text{solv}}}{I_{\max} - I_{\text{solv}}}, \quad (3)$$

where  $c_{\text{rel}}$  is the relative polymer concentration. The dependency of  $G'$  on the relative polymer concentration during polymerization is shown in Fig. 3a which follows a characteristic power law with a scaling of 2.3 based on the theoretical framework of polymer dynamics in semi-

dilute entangled polymer solutions.<sup>13</sup> The elastic response of semi-dilute entangled polymer solutions can be described by a random walk of correlation blobs with size  $\xi$  (distance to neighboring chains) representing the entanglement strand inside a confining tube with diameter  $a$ .<sup>13</sup> The confining tube is illustrated in Fig. 3b. Considering the concentration dependency of both the tube diameter and the size of the correlation blobs,  $G'$  can be described according to

$$G' = \frac{kT}{a^2 \xi} \sim c^{2.31} \quad (\text{good solvent}), \quad (4)$$

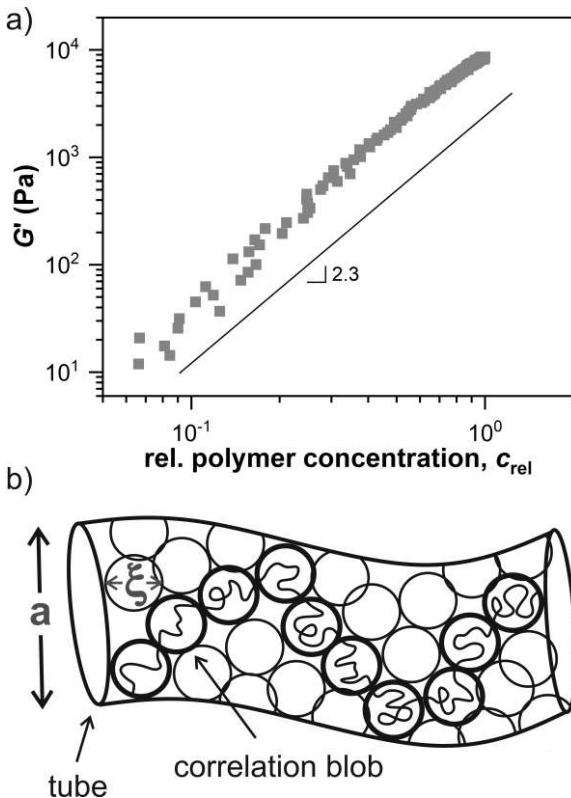


Figure 3. a) Relative polymer concentration dependency of  $G'$ , displayed on a log-log scale. Solid line is a guide to the eye that represents a power law with a scaling exponent of 2.3. b) Confining tube with diameter  $a$  and correlation length  $\xi$  in a semi-dilute entangled polymer solution. The random walk of correlation blobs describes the entanglement strand. Thin cycles represent the neighboring polymer chains.

which is in agreement with the found correlation of  $G'$  with  $c_{\text{rel}}$ . The prefactor of this power law corresponds to the maximum  $G'$  value ( $G'_{\text{max}}$ ). By combining Eq. 2 and Eq. 3,  $G'$  is a function of the NMR signal intensity according to

$$G'(t) = G'_{\text{max}} \left( \frac{t^m}{t^m + \theta_{\text{NMR}}^m} \right)^{2.3} \quad (5)$$

This relationship demonstrates that NMR can be used as a non-invasive concentration probe by employing a  $T_1$  filter that is adjusted towards chemical moieties along the polymer backbone while simultaneously suppresses solvent signal. In future studies, this approach will be used to elucidate the influence of solvent quality (theta solvent) and polymer structure such as polyelectrolytes with respect to the theoretical prediction of  $G'$ . An extended manuscript is currently in preparation that explores the influence of bivalent crosslinker on the nanoscopic structure.<sup>14</sup> Moreover, a particular emphasis will be the investigation of the strain dependency of  $T_2$  times. Since polymer chains are stretched and elongated during deformation, a reduction of  $T_2$  times as a function of strain can be expected.

## CONCLUSION

We present the use of a unique low-field RheoNMR device to study the gelation during AAC free radical solution polymerization. The gelation kinetics measured by both rheology and TD-NMR are directly in-situ correlated and reveal a characteristic inverse relationship between  $G'$  and  $T_2$  relaxation times. Moreover, we demonstrate a rather simple method to exploit TD-NMR measurements as a concentration probe by applying a  $T_1$  filter. This enables the quantification of the  $G'$  polymer concentration dependency, which shows a characteristic power law with an

exponent of 2.3 and confirms the theoretical prediction based on polymer dynamics in semi-dilute entangled polymer solutions.

#### ACKNOWLEDGEMENTS

CF acknowledges the Fonds der Chemischen Industrie (FCI) for funding via the Kekulé fellowship.

#### REFERENCES

- 1 H. Henning Winter. "Polymer Gels, Materials That Combine Liquid and Solid Properties." *MRS Bulletin* 16, no. 8 (1991): 44–48.
- 2 Gaynor M. Kavanagh, Simon B. Ross-Murphy. "Rheological Characterisation of Polymer Gels." *Progress in Polymer Science* 23, no. 3 (1998): 533–62.
- 3 Kay Saalwächter. "Microstructure and Molecular Dynamics of Elastomers as Studied by Advanced Low-Resolution Nuclear Magnetic Resonance Methods." *Rubber Chemistry and Technology* 85, no. 3 (2012): 350–86.
- 4 Johannes Höpfner, Gisela Guthausen, Kay Saalwächter, Manfred Wilhelm. "Network Structure and Inhomogeneities of Model and Commercial Polyelectrolyte Hydrogels as Investigated by Low-Field Proton NMR Techniques." *Macromolecules* 47, no. 13 (2014): 4251–65.
- 5 Karl-Friedrich Ratzsch, Christian Friedrich, Manfred Wilhelm. "Low-Field Rheo-NMR: A Novel Combination of NMR Relaxometry with High End Shear Rheology." *Journal of Rheology* 61, no. 5 (2017): 905–17.
- 6 Volker Röntsch, Mürüvvet Begüm Özen, Karl-Friedrich Ratzsch, Eric Stellmanns, Michael Sprung, Gisela Guthausen, Manfred Wilhelm. "Polymer Crystallization Studied by Hyphenated Rheology Techniques: Rheo-NMR, Rheo-SAXS, and Rheo-Microscopy." *Macromolecular Materials and Engineering* 304, no. 2 (2019): 1800586.
- 7 K. P. A. M. van Putte, J. den van Enden. "Pulse NMR as a Quick Method for the Determination of the Solid Fat Content in Partially Crystallized Fats." *Journal of Physics E: Scientific Instruments* 6, no. 9 (1973): 910–12.
- 8 Gisela Guthausen. "Analysis of Food and Emulsions." *TrAC Trends in Analytical Chemistry* 83 (2016): 103–6.
- 9 Terry Gullion, David B. Baker, Mark S. Conradi. "New, Compensated Carr-Purcell Sequences." *Journal of Magnetic Resonance (1969)* 89, no. 3 (1990): 479–84.
- 10 Saul Meiboom, D. Gill. "Modified Spin-Echo Method for Measuring Nuclear Relaxation Times." *Review of Scientific Instruments* 29, no. 8 (1958): 688–91.
- 11 Andreas Maus, Christopher Hertlein, Kay Saalwächter. "A Robust Proton NMR Method to Investigate Hard/Soft Ratios, Crystallinity, and Component Mobility in Polymers." *Macromolecular Chemistry and Physics* 207, no. 13 (2006): 1150–58.
- 12 Kay Saalwächter. "Proton Multiple-Quantum NMR for the Study of Chain Dynamics and Structural Constraints in Polymeric Soft Materials." *Progress in Nuclear Magnetic Resonance Spectroscopy* 51, no. 1 (2007): 1–35.
- 13 Ralph H. Colby. "Structure and Linear Viscoelasticity of Flexible Polymer Solutions: Comparison of Polyelectrolyte and Neutral Polymer Solutions." *Rheologica Acta* 49, no. 5 (2010): 425–42.
- 14 Christian Fengler, Jonas Keller, Karl-Friedrich Ratzsch, Manfred Wilhelm. "In-Situ RheoNMR Correlation of Polymer Segmental Mobility with Mechanical Properties During Hydrogel Synthesis." (*in preparation*).